International Journal of Computational Intelligence Systems, Vol. 8, Supplement 2 (2015), 28-40

Signal Feature Extraction Using Granular Computing. Comparative Analysis with Frequency and Time Descriptors Applied to Dynamic Laser Speckle Patterns

Ana L. Dai Pra
Grupo Inteligencia Artificial, Departamento de Matemática. Facultad de Ingeniería, Universidad Nacional de Mar del Plata
e-mail: daipra@fi.mdp.edu.ar

Lucia I. Passoni
Instituto de Investigaciones Científicas y Tecnológicas en Electrónica (ICyTE). Facultad de Ingeniería, Universidad Nacional de Mar del Plata.
e-mail: isabel.passoni@gmail.com

G. Hernan Sendra
Imaging Facility, Zentrum für Molekulare Biologie der Universität Heidelberg. Im Neuenheimer Feld 282, D-69221 Heidelberg, Germany
e-mail:ghsendra@gmail.com

Marcelo Trivi
UID Optimo, Dpto. Ciencias Básicas, Fac. Ingeniería, Universidad Nacional de La Plata. Centro de Investigaciones Opticas (CONICET La Plata - CIC)
e-mail: marcelot@ciop.unlp.edu.ar

Hector J. Rabal
Centro de Investigaciones Opticas (CONICET-CIC)
e-mail:hrabal@ing.unlp.edu.ar

Received 31 July 2015

Accepted 30 October 2015

Abstract

The laser dynamic speckle is a phenomenon caused by the fluctuant interference of the laser light reflected from an illuminated surface where some kind of activity is taking place. Signals generated by the intensity changes in each pixel through the sequence are processed with the finality of identifying underlying activity in each point. In this work we compare the performance of a Rough Fuzzy Granular Descriptor (previously published) against a set of dynamic speckle descriptors based in time and frequency processing. To perform this evaluation a numerical simulation is proposed to explore their linearity, robustness, sensitivity related to the samples quantity, as well as also by their computing time. Also the robustness to inhomogeneous spatial intensity was evaluated in an experiment performed with the illuminated surface of an actual biological object.

Keywords: Biospeckle, dynamic speckle simulation, rough-fuzzy sets.

1. Introduction

When an object surface, illuminated by a coherent beam, presents some type of local movement, the intensity and shape of the observed speckles evolve with time. The speckle patterns thus become time dependent. This phenomenon is also characteristic of biological samples and is known as biospeckle. The biospeckle activity is the consequence of microscopic movements or local changes in the refractive index of the sample properties.

Biospeckle patterns can be classified also as "boiling" patterns1 since the speckles move, deform, disappear and reappear without any significant displacement of their mean position1. This behavior can also be observed in some non-biological processes, such as drying of paints, corrosion, etc. Both, the time evolution of a pixel intensity and its spatial distribution over an image show seemingly random variations similar to those found in the height distributions of a rough surface. The characterization of rough surfaces requires the measurement of a considerable set of parameters. A similar behavior can be expected for speckle patterns, added to the fact that the inner dynamics of the process that produces them are most of times poorly known. Therefore many descriptors found in the literature are either heuristic or describe only some of the mechanisms.

Biological samples include many variables and show inherent variability; hence different contributions to dynamic speckle cannot easily be assigned.

Although many descriptors have been developed to characterize dynamic speckle, not all of them are suitable for all applications and there is no well defined criterion on how to make a choice. This work presents some approaches to analyze, compare and evaluate the Rough-Fuzzy Granular Descriptor (*RFGD*) vs. other descriptors on simulated series where it is possible to assess the awaited behavior when studying an application.

With this aim, a set of simulated speckle patterns was generated by using a numerical model that had been tested with actual experiments[2]. It is based on the simulation of an in-plane moving diffuser in pure boiling conditions; where the activity level varies according to the speed of the diffuser in a controlled way. The descriptors must provide numerical values highly correlated with the activity of the sample under study.

A group of the most commonly used descriptors were compared with *RFGD*: standard deviation, temporal contrast, full width at half maximum of autocorrelation, high to low ratio, cutoff frequency, Shannon entropy, wavelet entropy, energy of spectral band, averaged differences, generalized differences, weighted generalized differences and subtraction average.

To test efficacy and efficiency of the descriptors to discover the level of the activity of the sample through the speckle image sequences is proposed an evaluation in terms of linearity with respect to the diffuser velocity, convergence and performance against the required quantity of images required. The computational time was also compared among the descriptors. Finally, the robustness to intensity variations within the sample was evaluated in an actual and complex experiment where a non-visible bruise in apples was detected.

2. Methods

2.1. Controlled simulations

In order to evaluate the performance of different algorithms, a huge set of samples is required to ensure an acceptable statistical representation of certain situation. Experimentally obtained biospeckle samples are subject to inherent variability; in addition, repeatable samples require controlled environmental conditions. Alternatively, numerical simulations obtained with a model of generation of dynamic speckle can provide a better approach to analyze the performance of descriptors. There are several existing numerical models to simulate speckle patterns[3,4,5], from where we have chosen the model by Sendra et al., whose numerical model and required conditions for boiling observation are described in[2]. It adequately describes a simple and repeatable boiling experiment, namely the speckle pattern produced by an in-plane moving diffuser under adequate geometrical conditions of the observation system. This numerical experiment can be reproduced in practice[6].

When a speckle pattern is generated by the motion of a rigid diffuser under the most general conditions it is possible to observe two phenomena. The first is the translation of the pattern as a whole and consequently also the translation of each speckle grain. The other appears when grains speckle change their shape and eventually vanish or are created as the diffuser moves and is called boiling. Generally, both phenomena occur simultaneously; however, there are conditions for which it is possible to observe patterns of pure translation or pure boiling. Okamoto and Asakura[1] describe these conditions for the case of fully developed speckle patterns, in which the scattering centers in the diffuser are uncorrelated with each other and the diffuser moves with certain speed. They use the normalized autocorrelation of the space-temporal intensity function.

The samples used in this work were numerically simulated in pure boiling condition.

2.2. Experiment: bruised apple

To detect bruised apple regions a sequence of 500 whole field 300x300 speckles images from red delicious apples was obtained. The damage was caused by a controlled impact produced by letting fall a steel ball on the apple, which cannot be appreciated by visual inspection. The images were assembled into a three-dimensional array, hence 90,000 (300x300) series are processed[7]. Then, an image of the sample is constructed with the descriptor value of each series. The process enables the segmenting of regions with different bio-activity levels, essentially bruised and non-bruised zones. The speckled images were not obtained by free propagation but consisted in subjective speckle focused images formed by an objective (usually f = 50mm, f/# = 16). An expanded laser beam was used for the illumination and the CCD camera registered the image with Fraunhofer subjective speckle.

3. Descriptors

There are many descriptors defined in the literature commonly used to extract features from speckle patterns. A sub-set of them was selected as the most representative within each category for making the comparison against the *RFGD*. In the following, the variable X will be considered as the signal that represents the temporal evolution of the intensity of a point in the speckle pattern, with a quantity of samples given by N. Hence, x_i is the *i-th* individual element of the X time series, where *i: 1, ... N*.

Three categories of descriptors are proposed as they are based on: statistical analysis, processing in the frequency domain and processing in the time domain.

Note that in this study those descriptors that consume significant resources with a priori known computational complexity are not evaluated, like[8,9], since the aim is to achieve effective descriptors and using low computational resources.

3.1. Rough-Fuzzy Granularity Descriptor (RFGD)

The Rough-Fuzzy Granularity Descriptor, a computed within the time domain, is actually based in the Fuzzy Granular Descriptor (*FGD*) previously published, which quantifies the time intensity variations as fuzzy sets granules[10]. Next, the approach of Rough Set theory was introduced to define the intensity information granules and to adapt the algorithm to a real time implementation[11]. In order to facilitate the encoding of the intensity range in well-defined regions, given each fuzzy set, the approximations of the corresponding rough set are defined. Each granule of the X signal is defined as a sequence of elements belonging to the same rough set upper approximation $\overline{R}$ of three (k) fuzzy sets of intensity *{light, medium and dark},* the rough-set membership values are restricted to {0,1}. As the $\overline{R}_k$ sets are overlapped, such will be the case for the granules. The *RFGD* is computed as in Eq (1).

$$RFGD = \sum_{k=1}^{3} \left| suc_{n,k}\left(\overline{R}(x_n,k)\right)\right| / N, \text{ with n=2,3,...,N} \tag{1}$$

being

$$suc_{nk} = \begin{cases} 1 & \text{if } \overline{R}(x_{n-1},k) \text{ is true and } \overline{R}(x_n,k) \text{ is false} \\ 0 & \text{in other case} \end{cases} \tag{2}$$

suc_{nk} indicates the ending of a succession of the same level of intensity, and |.| indicates here cardinality, i.e., *RFGD* is the number of granules registered in N samples. The rough-fuzzy set parameters are obtained from the intensity histogram of a speckle pattern; tuning this characteristic to a particular sample acquisition.

3.2. Descriptors based on statistical analysis

3.2.1 Standard Deviation (SD)

From the statistical point of view, the simplest method to detect variations in a signal is the standard deviation (SD), which is a measurement of the variations in the time series with respect to the mean value [12, 13]

$$SD = \sigma(X) \tag{3}$$

3.2.2 Temporal Contrast (TC)

In actual experiments, the *SD* is related and thus very sensible to the mean intensity of the speckle pattern, since the speckle is not a linear process. A first way to solve this problem is the division of the *SD* by the mean intensity. In order to differentiate this descriptor from the spatial image contrast originally proposed by Briers[12], named “temporal contrast”.

$$TC = \frac{\sigma(X)}{\langle X \rangle} \tag{4}$$

where $\langle \cdot \rangle$ means temporal average.

3.2.3 Full Width Half Maximum of the Autocorrelation (FWHMA)

The first order statistics have the disadvantage of not taking into account the effect of the time lag between samples. In dynamic speckle signals, the autocorrelation function R_k, is usually a monotonically decreasing function expressed as:

$$R_k = \sum_{\cdot}^{\cdot\cdot} x_{n+k} x_n, \quad \text{where } 0 \le k \le N \tag{5}$$

A normalized version is typically employed, which is the result of dividing Eq (5) by R_0 (at 0 lag). Hence, *FWHMA* is computed as the lag of the R_k at its half maximum [14].

3.3. Descriptors based on frequency analysis

The information of a time-varying signal is usually better interpreted from the frequency point of view. The Fourier transform of the autocorrelation function is the Power Spectral Density (PSD), which can be also employed to describe signal activity.

Fig. 1 shows two intensity series of simulated speckle patterns at low and high velocities, together with their respective PSD estimation. In order to reduce artifacts in the Fourier transform due to the finite-length of the discrete signal, the PSD is computed using the Bartlett-Welch estimator [15].

The multispectral nature of the speckle signal and its analysis in the frequency domain give raise various descriptors of interest.

3.3.1 Energy of Spectral Band (ESB)

Under the hypothesis of the usefulness of the information provided by the spectrum, a descriptor is proposed based on the energy of the filtered signal. Sometimes, filtering the pattern intensity in the frequency domain helps to find a particular band that can characterize the boiling speckle. Infinite Impulse Response filters (IIR) are usually preferred to Finite Impulse Response (FIR) ones, given that a sharper transition region roll-off than FIR filter of the same order can be achieved. The descriptor is then computed as the energy of the previously filtered signal X [15].

$$ESB = \frac{1}{N} \sum_{n=1}^{N} x_n^{\,2} \tag{6}$$

There is no a priori method to know in which frequency band is the "useful" information of the signal. Although the *ESB* is also an empirical descriptor, an initial bank of filters can be applied to detect the bands of interest [16]. The *ESB* is the easiest analysis of the phenomena that originated the speckle signal. Finally, the High to Low Ratio (*HLR*) descriptor (see next section) can also be applied to relate two frequency bands.

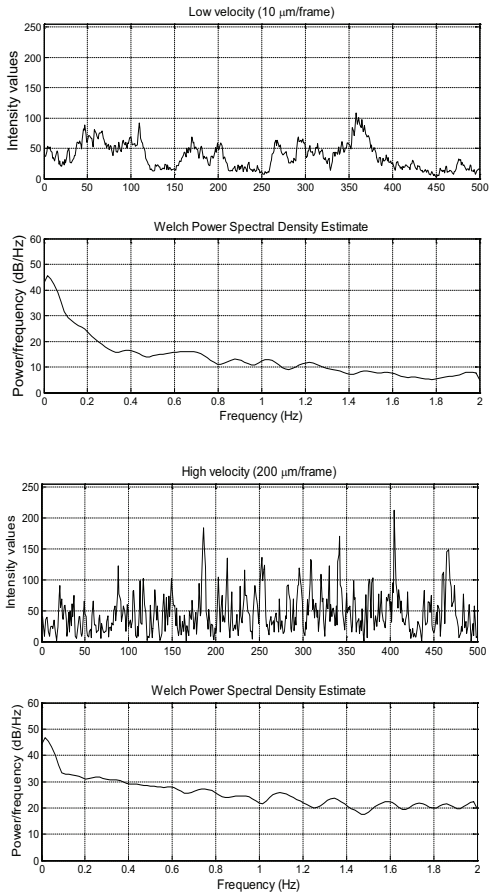

Fig. 1. Intensity series of simulated speckle patterns at low and high velocities

For the case of low frequency bands, a prior subtraction of the mean value of the signal ($\langle X \rangle$) is required. This descriptor has turned out to be also effective to characterize some processes under non-

uniform illumination, where each signal value is pre-processed with the following expression:

$$\tilde{x}_i = \left(x_i - \langle X \rangle\right) / \langle X \rangle \tag{7}$$

3.3.2 High to Low Ratio (HLR) of the Power Spectral Density

Fujii et al.[17] proposed the *HLR* of two empirically selected frequencies:

$$HLR = \frac{s_H}{s_L} \tag{8}$$

where s_H and s_L are the values of the PSD at a high and low frequency respectively.

Generally, s_L is computed within the interval from $f=0$ to $0.25\ f_{max}$ and s_H is computed from $0.25\ f_{max}$ to f_{max}. considering f_{max} as the maximum frequency of the PSD decomposition.

3.3.3 Mean Frequency (MF)

Another descriptor of the PSD is the mean frequency (*MF*) introduced by Aizu and Asakura[18], defined as

$$MF = \frac{\sum_{k=1}^{N_f} f_k s_k}{\sum_{k=1}^{N_f} s_k} \tag{9}$$

where s_k is the k-th component of the PSD and f_k its frequency value and N_f is equal to the total number of frequency components.

3.3.4 Cutoff Frequency (CF)

This descriptor computes the frequency at the half of the PSD maximum, hence this procedure is analogous to the *FWHMA*, but applied now to the PSD instead of the autocorrelation [18]

3.3.5 Shannon Entropy (SE) of the Power Spectrum Density

An alternative descriptor of the PSD is the entropy introduced originally by Shannon as a measure of the signal "disorder"[19]. The spectral entropy value is obtained multiplying the PSD estimate [*Pf(X)*] by its natural logarithm [$log_e Pf(X)$], summed over all f frequency components. Thereafter, the entropy value is normalized to range between 1 (maximum irregularity) and 0 (complete regularity) [20]. The value is also divided by the maximum of the spectrum entropy of N_f samples (log N_f) where N_f is equal to the total number of frequency components and is mathematically expressed as:

$$SE = \frac{-\sum_{f=1}^{N_f} \frac{s_f}{S} \log\left(\frac{s_f}{S}\right)}{\log(N_f)} \tag{10}$$

where s_f is the f-th element of the power density spectrum vector **s** of length N_f, and S is

$$S = \sum_f s_f \tag{11}$$

3.3.6 Discrete Wavelet Transform Entropy (DWTE)

Instead of using *PSD*, the Shannon Entropy can also be applied to the decomposition of the signal using the *DWTE*[21,22,23,24]. *DWTE* makes no assumptions about signal stationary feature[7], so it provides a useful tool for the frequency analysis considering the temporal location[23]. This feature makes it possible to compute the time evolution of its entropy as a measure of the variation of the complexity or disorder of the time series. The wavelet transform (*WT*) is the representation of a signal X by means of its inner products with a set of basic wavelet functions.

A wavelet family $\psi_{a,b}$ is the set of functions generated by dilations and translations of a unique admissible mother wavelet $\psi(t)$

$$\psi_{a,b}(t) = |a|^{-1/2} \psi\left(\frac{t-b}{a}\right) \tag{12}$$

where $a,\ b \in \boldsymbol{R},\ a \neq 0$ are the scale and translation parameters respectively and t is time. The wavelet becomes narrower accordingly as a decreases. WT provides a tool for simultaneously observing a time series at a full range of different scales a, while retaining the time dimension of the original data. Multi-resolution analysis theory shows that no information is lost if the continuous wavelets coefficients are sampled at a sparse set of points in the scale-time plane known as the dyadic grid. This grid leads to the *DWTE*, where the scale parameter is $a_j=2^{-j}$ and the translation $b_{j,k}=2^{-j}k$, with $j,k \in$ Z.

If the signal is assumed to be given by a set of sampled values corresponding to an uniform time grid, carrying out the decomposition over all resolution levels $M=log_2(N)$, the wavelet expansion will be:

$$S(t) = \sum_{j=0}^{\infty} \sum_{k} C_j(k) \psi_{j,k}(t) = \sum_{j=0}^{\infty} r_j(t) \qquad (13)$$

where $C_j(k)$ can be interpreted as the local residual errors between successive signal approximations at scales j and $j+1$ and $r_j(t)$ is the residual signal at scale j. The energy at each resolution level $j=-1,\ldots,-M$. ($M=log_2(N)$), will be the energy of the detail signal, at a given time window.

In order to study the time evolution of the speckle pattern, signal X is divided into temporal windows i of length L The following expression is used to obtain the mean wavelet energy of the detail signal j at each time window i

$$E_j^{(i)} = \sum_{k=0}^{(L/2^j)-1} \left| C_{k,j,i} \right|^2 \qquad (14)$$

with (i=1,…,NT, with $NT=N/L$, The total energy at interval i can be obtained by:

$$E_{total}^{(i)} = \sum_{j<0} E_j^{(i)} \qquad (15)$$

The signal window i relative wavelet energy will be given by:

$$p_j^{(i)} = \frac{E_j^{(i)}}{E_{total}^{(i)}} \qquad (16)$$

The following expression is used to evaluate the window i Shannon entropy[22]. The obtained value is assigned to the central window point, normalized with the log of the maximum level of decomposition, to obtain entropy values in the [0,1] interval.

$$DWTE = \frac{-\sum_{j<0} p_j \cdot \log\left[p_j\right]}{\log M} \qquad (17)$$

Consequently if the embedded behavior changes of the intensity series can be characterized by the time evolving entropy value, this parameter can be considered as a descriptor of the dynamic biospeckle. This descriptor has been successfully applied to the assessment of time varying phenomena like the paint drying of acrylic enamel [7].

3.4. Descriptors based on Time Domain Analysis

The following descriptors are based on the time domain calculations; hence, they strongly depend on the number of signal samples. In order to avoid this effect, a normalization division by the quantity of samples (N) was included in their mathematical expressions.

3.4.1 Averaged Differences (AD)

Due to the non-linearity of the speckle phenomenon, the mean intensity value is not suitable to weight the standard deviation. An alternative approach was introduced by Fujii et al [25,26], called *Averaged Differences* and also known as Fujii's descriptor. Here the difference between contiguous samples is weighted by the local average by the following expression:

$$AD = \sum_{n=2}^{N} \frac{\left| x_n - x_{n-1} \right|}{\left| x_n + x_{n-1} \right|} / N \qquad (18)$$

where |.| indicates absolute value.

3.4.2 Generalized Differences (GD)

Although the *AD* descriptor is very suitable for many applications, it suffers of two disadvantages: it is very sensible to the noise in regions of low intensity values and it is not suitable to detect slow varying speckle signals. In order to adapt it to these situations, a descriptor called Generalized Differences was presented by Arizaga et al [27], where intensity variations in different time scales are taken into account using the following expression:

$$GD = \left(\sum_{n} \sum_{l} \left| x_n - x_{n+l} \right| \right) / N \qquad (19)$$

where n and l are indices spanning all the possible numbers of the registered images. As every x_n value is subtracted from every other value in X, the result does not depend on the sequence. This descriptor is thus very sensitive to the number of samples.

3.4.3 Weighted Generalized Differences (WGD)

An additional parameter $\boldsymbol{p}$ was later added to the *GD* descriptor with the aim of controlling its sensitivity. The elements of this vector allow giving different weights according to the gap of each subtraction.

$$WGD = \left(\sum_{n=1}^{N-p} \sum_{l=1}^{p} \left| x_n - x_{n+l} \right| p_l \right) / N \qquad (20)$$

The resulting descriptor, called Weighted Generalized Differences (*WGD*), was found useful to detect different types of activities. However, the

selection of parameter p is highly empirical and limits its application from the practical point of view.

3.4.4 Subtraction Average of consecutive intensities (SA)

One of the simplest descriptor is the Subtraction Average (*SA*) of two consecutive elements of the *X* time speckle pattern [28].

$$SA = \sum_{n=1}^{N-1} |x_n - x_{n+1}| / N - 1 \tag{21}$$

4. Results and discussion

4.1. Controlled Simulations

Sets of images with different controlled activities were simulated by using different speeds of the moving diffuser and applied as input to the different descriptors. Velocities from 1 to 200 in steps of 2 *μm/frame* were considered, and a set of 2000 samples of 512x512 pixels were obtained for each velocity.

Since the objective is to measure the level of activity of the sample through the speckle activity, the proposed descriptors are computed under different simulations setups. Descriptors are expected to be effective in discovering the dynamics of the sample, to that end will be assessed:

-*The evolution of the value of the descriptors with the rate of change of the sample (simulated with the speed of the diffuser)*. To show the comparison of the computed descriptors mean values of the 512 series are plotted for each experiment. Standard deviations are not shown on the same graphics in order not to mask visualization among different setups. Results corresponding to 512 (*X*) time series of 50, 200, 500, 1000 and 2000 samples were obtained. They are plotted against the simulated speed of the diffuser in micrometers per frame (Fig. 2 to 14).

-In Table 1 a set of computed features is shown to compare descriptors performances according to the number of images used. Hence, for each descriptor are shown the Variation Coefficient C_d, the Linear Correlation Coefficient r_{vd}, the Sensitivity of the Descriptor, s_{di} and the Computing Time applied to different samples quantity.

-*Linear Correlation Coefficient*: in order to quantitatively assess the linearity of the descriptor in relation to the speed of the diffuser, the linear correlation coefficient is calculated. The Pearson's linear correlation coefficient shows a statistical relationship between the descriptor and the diffuser velocity values. It is defined as

$$r_{vd} = \frac{\sum_{i=1}^{L} (v_i - \langle v \rangle)((d_i - \langle d \rangle)}{(L-1)\sigma_v \sigma_d} \tag{22}$$

where v is the diffuser velocity value, d is the descriptor value, L is the number of considered velocities, σ are the standard deviations and, $\langle v \rangle$ and $\langle d \rangle$ stand for v and d means respectively.

-*Variation coefficient*: as the descriptor standard deviation is not plotted, the C_d is computed to show the extent of variability in relation to the mean computed over the 512 values. It is defined as the ratio of the standard deviation σ_d to the mean $\langle d \rangle$ of the descriptor variable d:

$$C_d = \frac{\sigma_d}{\langle d \rangle} \tag{23}$$

-*Sensitivity of the Descriptor*, s_{di}, is the relative difference between the value obtained using i samples (d_i) and 2000 samples (d_{2000})

$$s_{di} = \frac{|d_i - d_{2000}|}{d_{2000}} \tag{24}$$

This coefficient is used to evaluate the relative difference among the results obtained with different samples number.

-*Computing Time* (*CT*) is the average of the elapsed time in processing each series in seconds.

As hypotheses can be stated that a good descriptor is one which exhibits linear response with respect to the rates of change of the sample (high correlation coefficient r_{vd}). The computed values should have low dispersion relative to its estimated value (low C_d), alse they must be independent of the number of images used for its calculation (low s_{di}). and the computing time (*CT*) should be low, making it liable to operate in near real time processes.

Figure 2 shows the *SD* as a function of the speed of the diffuser. In all cases the descriptor was asymptotic to the same value. This descriptor can be useful only to describe low speeds and requires only a small number

of samples. Results of *TC* descriptor (Fig. 3) are quite similar to *SD*, showing less noisy tendency than the *SD*.

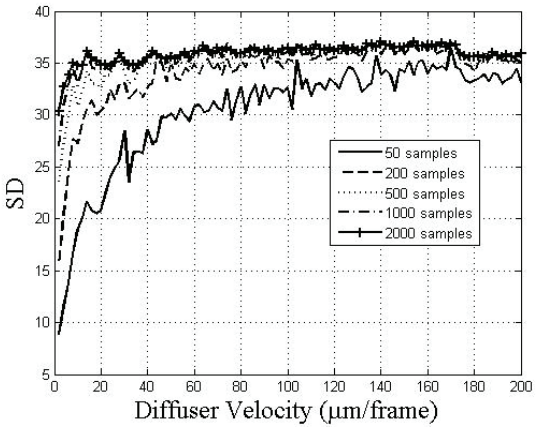

Fig. 2. Standard Deviation descriptor (*SD*)

Fig. 4 shows that *FWHM* can distinguish speeds up to 60 μm/frame diffuser in our experiment. Above that value, changes in activity are indistinguishable via this descriptor.

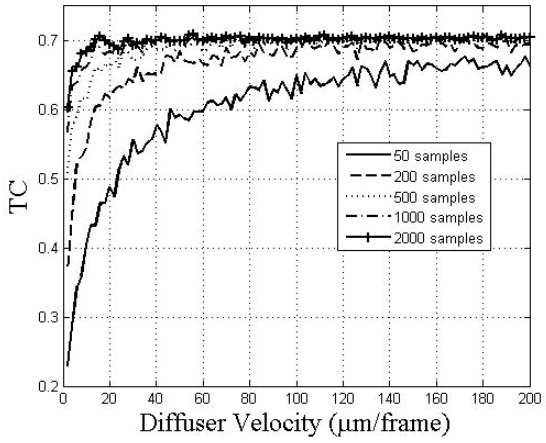

Fig. 3 Temporal Contrast desdriptor (*TC*)

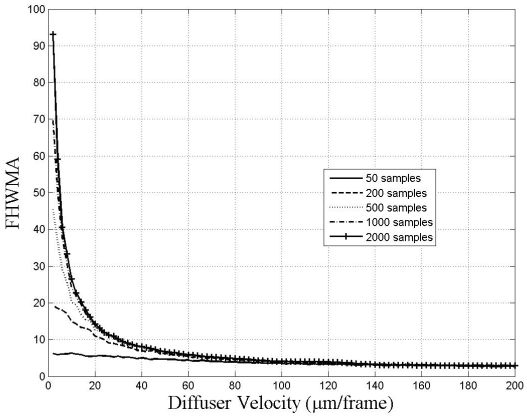

Fig.4: Full Width Half Maximum of the Autocorrelation (*FHWMA*)

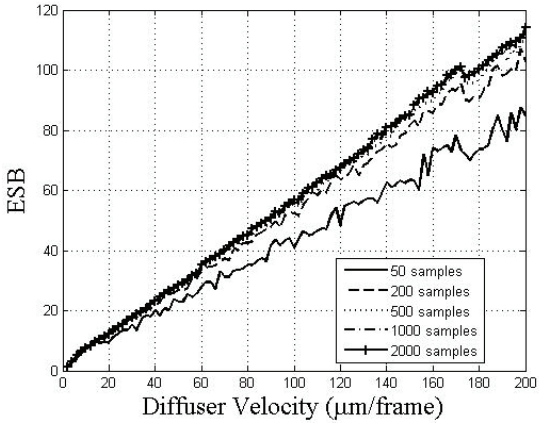

Fig.5 Energy of spectral bands descriptor

The Energy of band pass filter (0.25 Hz to 5Hz) is exhibited in Fig. 5. The losses specification in each of this filters are the following: maximum tolerated at the pass band 1db and the minimum losses required at the reject band is the 40db. Elliptic approximation (Cauer) filters were used because, in spite of their higher implementation complexity, they exhibit a more selective frequency response than Butterworth solution.

It is observed an acceptable linearity behavior with the *HLR* (Fig. 6) highly independent of the number of images as exception of the experiment that uses only 50 samples.

The *MF* (Fig. 7) shows also an acceptable linearity with the diffuser velocity; with very similar values when more than 200 samples are computed.

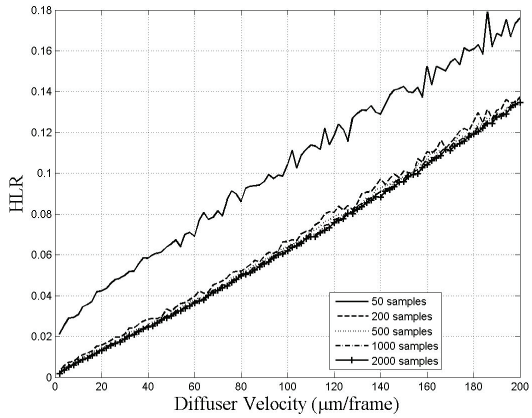

Fig. 6 High-Low Ratio descriptor (*HLR*)

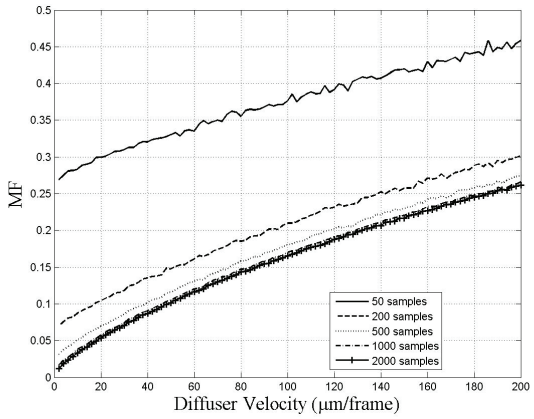

Fig.7 Mean Frequency descriptor (*MF*)

Descriptors at Fig. 8 (*CF*), Fig. 9 (*SE*) and Fig. 10 (*DWTE*, computed using Daubechies db8) exhibit high dependency with the samples quantity. *SE* and *DWTE* descriptors do not discriminate as well as *ESB, HLR*, and *MF* higher velocities than 50 μm/frame.

Fig. 11 shows the *AD* as a function of the diffuser speed. It can be seen that the trends show no appreciable noise. An advantage of this descriptor is its ability to differentiate a far wider range of activities.

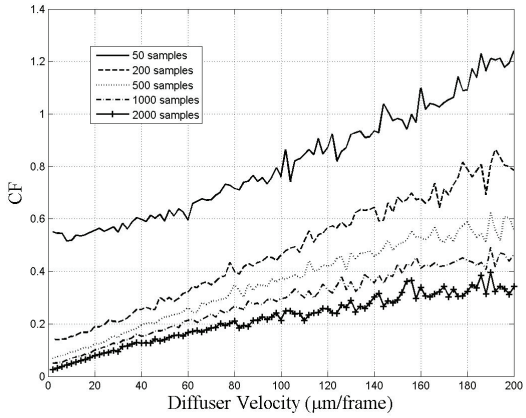

Fig.8: Cut-off frequency descriptor (*CF*)

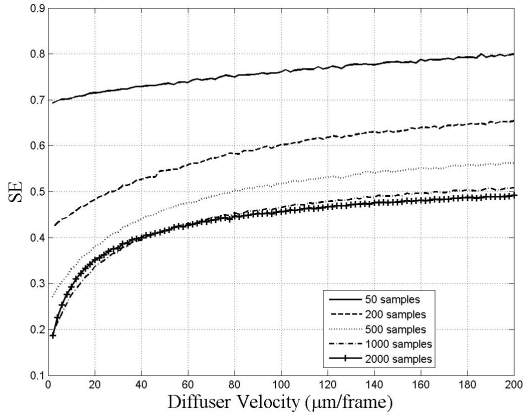

Fig. 9 Shannon Entropy descriptor (*SE*)

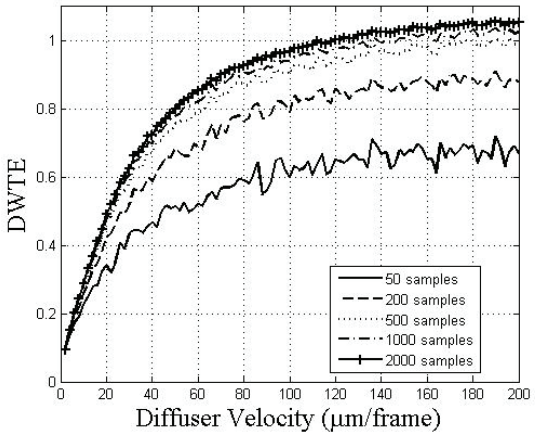

Fig. 10 Discrete Wavelet Transform Entropy (*DWTE*)

Fig. 12 can be observed *GD* as a constant function of the diffuser speed; hence it is not appropriate to characterize the activity of pure boiling patterns generated by the displacement of a diffuser. This undesirable behavior is overcome with the *WGD* descriptor showed in Fig. 13.

The *RFGD* linearity (Fig. 15) is comparable with the *SA* (Fig. 14), the *AD* (Fig. 11) and *WGD* using *p=5* (Fig. 13).

The descriptors that exhibit less dependency to the number of samples are *AD, SA* and *RFGD*, followed by *ESB* and *HLR*. It can be appreciated in the graphs as overlapped curves for different amount of used samples.

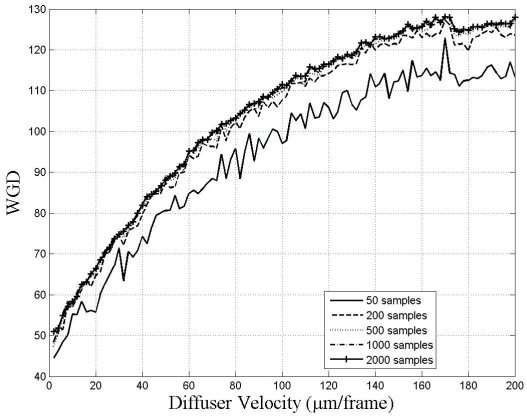

Fig. 13 Weighted Generalized Differences descriptor (*WGD*)

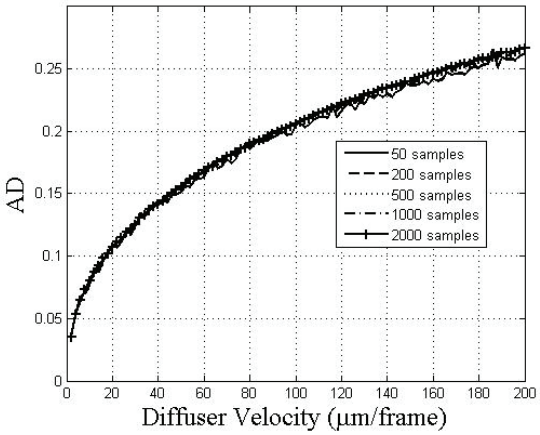

Fig.11 Average Differences descriptor (*AD*)

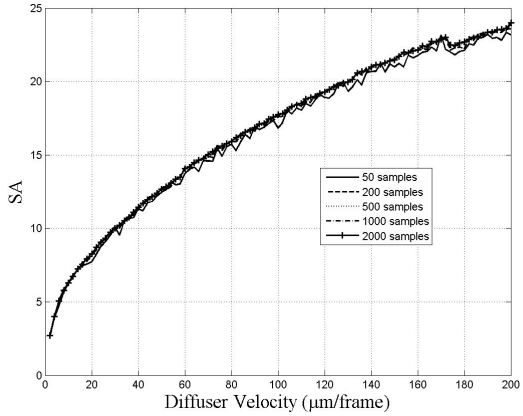

Fig. 14 Subtraction Average descriptor (*SA*)

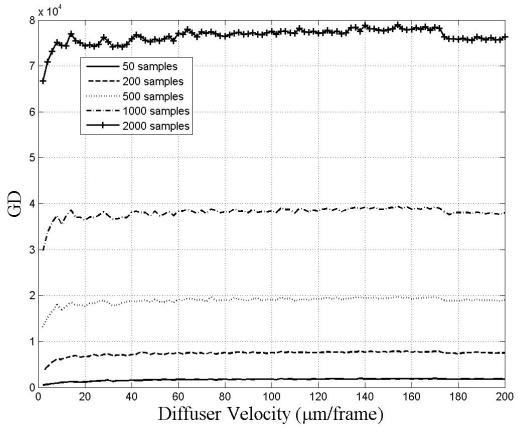

Fig.12 Generalized Differences descriptor (*GD*)

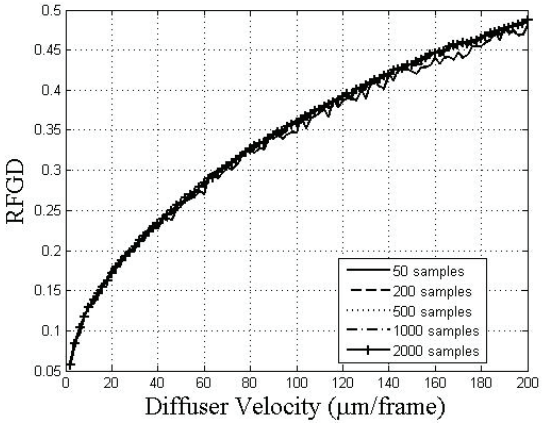

Fig. 15: Rough Fuzzy Granular descriptor (*RFGD*)

Table 1. Correlation, Variation coefficient, Sensitivity and Computing Time average

Descriptor	Correlation coefficient r_{vd} Quantity of images					Variation coefficient C_d Quantity of images					Sensitivity s_{di} Quantity of images				Computing time average CT [s] Quantity of images				
	50	200	500	1000	2000	50	200	500	1000	2000	50	200	500	1000	50	200	500	1000	2000
SD	0.794	0.65	0.601	0.545	0.537	0.318	0.19	0.131	0.095	0.069	0.156	0.051	0.021	0.009	0.001	0.002	0.004	0.011	0.026
TC	0.792	0.648	0.599	0.524	0.437	0.21	0.124	0.084	0.062	0.045	0.139	0.047	0.018	0.007	0.001	0.002	0.005	0.013	0.03
FWHMA	0.953	0.794	0.664	0.592	0.544	0.26	0.202	0.148	0.115	0.088	0.234	0.095	0.044	0.018	0.115	0.145	0.196	0.304	0.588
ESB	0.996	0.998	0.999	0.999	0.999	0.579	0.285	0.185	0.135	0.103	0.217	0.062	0.023	0.01	0.485	0.499	0.536	0.616	0.757
HLR	0.997	0.999	0.999	0.999	0.999	0.308	0.245	0.174	0.119	0.087	1.096	0.102	0.046	0.021	1.179	1.305	1.190	1.334	1.429
MF	0.995	0.994	0.993	0.992	0.992	0.090	0.097	0.086	0.066	0.050	2.236	0.468	0.150	0.037	1.181	1.304	1.188	1.330	1.424
CF	0.984	0.994	0.988	0.986	0.975	0.354	0.397	0.474	0.500	0.631	3.578	1.258	0.651	0.312	1.188	1.315	1.200	1.343	1.440
SE	0.986	0.948	0.904	0.875	0.852	0.024	0.034	0.04	0.036	0.028	0.777	0.351	0.132	0.026	1.187	1.310	1.195	1.336	1.433
DWTE	0.862	0.858	0.854	0.848	0.845	0.398	0.212	0.126	0.084	0.055	0.345	0.156	0.059	0.026	0.695	0.697	0.714	0.767	0.866
AD	0.963	0.964	0.964	0.964	0.964	0.182	0.097	0.062	0.045	0.032	0.021	0.008	0.004	0.003	0.001	0.004	0.013	0.033	0.068
GD	0.77	0.611	0.57	0.519	0.527	0.309	0.180	0.122	0.088	0.064	0.978	0.904	0.754	0.503	0.007	0.155	1.310	8.441	35.355
WGD	0.946	0.947	0.949	0.949	0.949	0.282	0.149	0.096	0.069	0.051	0.977	0.902	0.752	0.501	0.001	0.002	0.005	0.013	0.054
SA	0.974	0.974	0.975	0.975	0.975	0.201	0.109	0.072	0.054	0.043	0.023	0.008	0.005	0.004	0.001	0.002	0.005	0.014	0.028
RFGD	0.974	0.975	0.975	0.975	0.976	0.209	0.108	0.070	0.050	0.037	0.021	0.007	0.004	0.002	0.006	0.023	0.057	0.113	0.225

The ability of the descriptors to identify the dynamics of the process is evaluated with the correlation coefficient rvd. High coefficients indicate a

linear relationship with the simulated velocity. As is observed in Table 1 this condition is fulfilled in both temporal (*AD, WGD, SA, RFGD*) and frequency descriptors (*ESB, HLR, MF, CF, SE, DWTE*) though not in the statistics ones (*SD, TC* and *FWHMA*) neither in the GD.

A low C_d is expected when defining a descriptor; this fact implies high reliability in its use. In Table 1 C_d, goes down with the increase of the number of samples, with exception of *CF*. *CF* shows the higher C_d, which makes it rather unreliable. The shadowed cells shows the best abilities in both features ($r_{vd} \geq 0.95$and $C_d < 0.1$).

The sensitivity S_{di} shows the capability of the descriptor d to get a good performance still using a low quantity of samples *i*. The shadowed cells shows the best performances in both features (S_{di} and $CT < 0.1$)

Evaluating Table 1 results we observe that *RFGD* shows similar performance to the *AD* and *SA* descriptors, all of them computed within the time domain (light brown shadowed).

4.2 Experiment: bruised apple

In order to assess the robustness of the descriptor to intensity variations in an area of the sample due to its topological characteristics, we evaluated the behavior of the descriptors in an actual and complex experiment where non-visible a bruise in apples was detected [7].

The goal was the recognition of the region bruised amid the healthy one. To compare their performance the Receiver Operator Characteristics (ROC) was used [29], and the area under the curve (AUC) was computed as a quality index. The descriptors were obtained using two different ensembles: of 500 and 50 images each. As is widely known, the AUC higher value the better the classifier.

In Table 2 the AUC values for each descriptor are shown in descending order. Using 500 samples the descriptor with the best performance with the higher AUC is the *RFGD* with 0.954, followed by the frequency descriptor *MF, HLR, ES, DWTE, CF* and *ESB* with values above 0.75. Other descriptors show an inadmissible performance with values below 0.5; in consequence they are not advisable to apply on samples with inhomogeneous spatial intensity. When a set of 50 images was used to compute the descriptors, no majors differences are shown in the *RFGD* performance, followed by the frequency ones. Nevertheless the *TC* and the *FWHMA*, both based on statistical analysis, enhance their performance in relation with that shown with 500 samples.

Table 2. Comparative graphs of the four evaluated features

	AUC	
Descriptor	500 samples	50 samples
RFGD	0 .954	0.940
MF	0 .936	0.902
HLR	0 .926	0.910
ES	0.896	0.895
DWTE	0.887	0.692
CF	0.862	0.830
ESB	0 .754	0.651
TC	0.412	0.718
FWHMA	0.276	0.667
AD	0.276	0.276
WGD	0.020	0.261
SA	0.019	0.410
SD	0.026	0.260

5. Conclusions

We have compared the performance of the *RFGD* versus several biospeckle descriptors by applying them to controlled numerical simulations and also to an actual experiment with non-visible bruises in apples. The performance evaluation for the numerical simulation of a controlled pure boiling speckle experiment was shown on plots of the descriptor value as a function of the diffuser simulated speed. The effect of changing the sample quantities, its convergence, linearity and the variation coefficient were also assessed.

It should be noted that most of the descriptors need to have a priori the total set of samples, e.g.: those based in frequency and statistics meanwhile those as *AD, SA* and *RFGD* could be computed as new samples appear. This latter feature makes them candidates to be embedded in real-time processes.

Thus, in the simulated experiment the set of descriptors based on statistical and *GD* do not have an acceptable coefficient of correlation. The coefficient of variation is acceptable for most experiments descriptors for over 500 samples except *CF* whose variability is high relative to the average. The descriptors based on frequency analysis as *MF, CF, SE*, and *DWTE* and also *GD* and *WGD* show high sensitivity to the number of samples used. The computation time is high for descriptors based on frequency analysis and also for the *GD* descriptor.

The result of the actual experiment shows that *RFGD* exhibits the best performance, followed by those based on frequency analysis, demonstrating that are robust to spatial changes of intensity within the sample, in agreement with the correlation analysis in the simulations.

Acknowledgements

This work was supported by CCT La Plata Consejo Nacional de Investigaciones Científicas y Técnicas (CONICET). Comisión de Investigaciones Científicas de la Provincia de Buenos Aires. by Facultad de Ingenieria. University of La Plata and by a Grant PICT 2008-1430. Agencia Nacional de Promoción de la Ciencia y la Técnica. Argentina.

References

1. Okamoto T, Asakura T. The statistics of dynamic speckles. Prog. Optics 1995; 34. 183-248
2. Sendra GH, Rabal H, Triv M, Arizaga R. Numerical model for simulation of dynamic speckle reference patterns. Optics Comm. 2009. 282 (18). 3693-700
3. Rabal H, Arizaga R, Cap N, Grumel E, Trivi M. Numerical model for dynamic speckle: an approach using the movement of scatterers. Journal of Optics A: Pure and Applied Optics. 2003; S381- S385.
4. Equis S, Jacquot P. Simulation of speckle complex amplitude: advocating the linear model. En Speckle06: Speckles, From Grains to Flowers. International Society for Optics and Photonics, 2006. p. 634138-634138-6.
5. Federico A, Kaufmann GH, Galizzi GE, Rabal H, Trivi M, Arizaga R. Simulation of dynamic speckle sequences and its application to the analysis of transient processes. Optics Comm. 2006; 260. 493-9
6. Sendra GH, Rabal H, Arizaga R, Trivi M. Vortex analysis in dynamic speckle images. JOSA A. 2009; 26(12). 2634-639
7. Passoni LI, Dai Pra AL, Rabal H, Trivi, Arizaga R. Dynamic speckle processing using wavelets based entropy. Opt Commun 2005; 246. 219-228
8. Guzmán MN, Hernán Sendra G, Rabal HJ, Trivi M. Island analysis of low activity dynamic speckles, 53 (1), 14-21, (2014). Appl Opt. 2014 Jan 1;53(1):14-21. doi: 10.1364/AO.53.000014.
9. López-Alonso JM, Alda J, Rabal H, Grumel E, Trivi M. Dynamic speckle analysis using multivariate techniques J. Opt. 2015; 17 (3). 035609 (7pp)
10. Dai Pra AL,Passoni LI, Rabal H. Evaluation of Laser Dynamic Speckle Signals Applying Granular Computing. Signal Process. 2009; 89(3). 266-274.
11. Todorovich E, Dai Pra AL, Passoni LI, Vázquez M, Cozzolino E, Ferrara F, Bioul, G. Real-time speckle image processing. Journal of Real-Time Image Processing, 2013; 1-11.
12. Briers D, Duncan DD, Hirst E, et al; Laser speckle contrast imaging: theoretical and practical limitations. J. Biomed. Opt. 2013; 18(6):066018-066018.
13. Briers J D. A note on the statistics of laser speckle patterns added to coherent and incoherent uniform background fields and a possible application for the case of incoherent addition. Optical and Quantum Electronics. 1975; 7 Short Communication.
14. Rabal H, Arizaga R, Cap N, Trivi M, Romero G, Alanís E. Transient phenomena analysis using dynamic speckle patterns. Opt. Eng. 1996; 35 (1). 57-62.
15. Passoni LI, Sendra GH, Arizmendi CM. Frequency Analysis . In: Rabal H, Braga RA Editors. Dynamic Laser Speckle and Applications. CRC Press Taylor & Francis Group. 2009. ISBN-13: 978-1420060157.
16. Murialdo SE. Passoni LI. Guzman MN. Sendra GH. Rabal H. Trivi M. Gonzalez JF. Discrimination of motile bacteria from filamentous fungi using dynamic speckle. J Biomed Opt. 2012. 17(5). 056011. doi: 10.1117/1.JBO.17.5.056011.

17. Fujii H, Asakura T, Nohira K, Shintomi Y and Ohura T .Blood flow observed by time-varying laser speckle. Optics Letters. 1985; 10 (3) 104-6 http://dx.doi.org/10.1364/OL.10.000104
18. Aizu Y, Asakura T. Bio-speckle phenomena and their application to the evaluation of blood flow. Opt Laser Technol 1991; 23(4). 205-19.
19. Shannon CE. A Mathematical Theory of Communication. Bell System Technical Journal 1948; 27 (3): 379–423.
20. Viertio-Oja H, Maja V, Sarkela M et al. Description of the entropy algorithm as applied in the Datex-Ohmeda S/5 Entropy Module. Acta Anaesthesiol Scand . 2004; 48: 154–61.
21. Blanco s, D'Attellis C, Isaacson S, Rosso O, Sirne R.Time-frequency analysis of electroencephalogram series (II): Gabor and wavelet transform. Phys Rev. E. 1996; 54. 6661-72.
22. Rosso O, Blanco S,Yordanova J, Kolev V, Figliola A, Schürman M, Basar E. Wavelet entropy: a new tool for analysis of short duration brain electrical signals. J Neurosc Meth 2001; 105. 65-75.
23. Braga RA, Horgan GW, Enes AM, Miron D, Rabelo GF, Barreto Filho JB. Biological feature isolation by wavelets in biospeckle laser images, Computers and Electronics in Agriculture, me 2007 ;58(2). 123-132
24. Ribeiro KR Jr. Sáfadi T. and Horgan G. Comparison between Fourier and Wavelets Transforms in Biospeckle Signals. Applied Mathematics. 2013;. 4(11) 11-22. doi: 10.4236/am.2013.411A3003.
25. Fujii H, Nohira K, Yamamoto Y, Ikawa H, Ohura T. Evaluation of blood flow by laser speckle image sensing. Part 1. Appl Optics 1987; 26(24). 5321-25.
26. Ribeiro K M, Barreto B, Pasqual M, White PJ, Braga RA, Dupuy LX, Continuous, high-resolution biospeckle imaging reveals a discrete zone of activity at the root apex that responds to contact with obstacles. Ann Bot. 2013 doi: 10.1093/aob/mct271
27. Arizaga R, Cap N, Rabal H, Trivi M. Display of local activity using dynamical speckle patterns. Opt Eng 2002; 41(2). 287-94
28. Braga Jr. R, Silva B, Rabelo G, Marques R, Enes A,; Cap N, Rabal H,Arizaga R, Trivi M, Horgan G. Reliability of biospeckle image analysis. Optics and lasers in engineering . 2007; 45(3) 390-95.
29. Ortiz CC, Sendra GH, Rabal HJ, Arizaga R, Trivi M. Dynamic speckle algorithms comparison using receiver operating characteristic. Opt Eng 2008; 47(05). 057005. 1